Calorimetric study of the magnetic order in $Ho(Co_{1-x}Rh_x)_2$ alloys

L. L. Henry and L. E. Wenger
Department of Physics, Wayne State University, Detroit, Michigan 48202

G. D. Khattak and A. Tari
Department of Physics, University of Petroleum and Minerals, Dhahran 31261, Saudi Arabia
(Received 29 May 1990)

Calorimetric measurements have been performed on a series of cubic Laves-phase compounds $Ho(Co_{1-x}Rh_x)_2$ for $x=0.02$, 0.05, 0.08, 0.12, 0.16, and 0.25. The heat-capacity data show first-order-type peaks at the ferromagnetic transition temperature T_C for concentrations with x values between 0.02 and 0.08. For larger concentrations, the peaks at T_C are much broader and more suggestive of a second-order transition. Utilizing the "*s-d*" model in conjunction with the specific-heat data suggests that the change from first to second order in the ferromagnetic transition for $x \geq 0.10$ is due to a reduction in the magnetic exchange interactions between the Ho $4f$ moments and the cobalt $3d$ electrons. In addition, the calorimetric data for $x \leq 0.16$ show another first-order peak at a lower temperature T_{sf} that can be associated with a change in the easy-magnetization direction of the Ho moments.

I. INTRODUCTION

In the RCo_2 (R being a rare-earth element) compounds, the magnetism cannot be adequately explained solely by the itinerant electron model. Instead, the coexistence of the $3d$ electrons from the cobalt atoms and of the localized spins from the rare-earth ions is necessary to provide a satisfactory description of the first-order ferromagnetic phase transition that results in $DyCo_2$, $HoCo_2$, and $ErCo_2$ with ferromagnetic Curie temperatures T_C less than 200 K and of the second-order ferromagnetic phase transition in $GdCo_2$ and $TbCo_2$ with $T_C > 200$ K.[1] In $HoCo_2$, the first-order ferromagnetic transition occurs at 75 K,[2] and is associated with exchange effects due to the Ho ions which induce a magnetic moment of $1.0\mu_B$ per cobalt atom.

In recent studies by Tari[3] on $Ho(Co_{1-x}Ni_x)_2$ compounds and by Hien, Duc, and Franse[4] on $Ho(Co_{1-x}Cu_x)_2$ compounds, the effect of substituting Ni and Cu for Co upon the nature of the ferromagnetic phase transition was studied. It was found that the phase transition in both systems was first order for $x \leq 0.1$ and second order for $x > 0.1$. This change from first to second order in these systems was interpreted within the framework of the "*s-d*" model.[5] For the $Ho(Co_{1-x}Ni_x)_2$ system, the change in order was caused by a reduction in the exchange field between the spin of the $3d$ electrons of the Co and the localized spin of the Ho ion. However, the disappearance of the first-order transition in the Cu-substituted $HoCo_2$ was explained in terms of an approximate 30% decrease in the paramagnetic susceptibility of the itinerant $3d$ electrons as the Cu concentration increased above $x=0.1$.

Since rhodium and cobalt are isoelectronic, the substitution of Rh for Co in $HoCo_2$ should provide a simpler system for the study of the magnetic phase transition in terms of its change in character (order) and the causes for the change. Because of the isoelectronic nature of Rh and Co, a large decrease in the paramagnetic susceptibility is not anticipated and thus the exchange field should be the more dominant interaction in determining the magnetic properties. More recently, Tari[6] has reported systematic magnetization studies on the effect of Rh substitution in $HoCo_2$. The magnetization change around T_C became progressively more gradual with increasing Rh concentration. A change in the order was deduced to occur at approximately 10 at. % Rh and was attributed to a reduction in the exchange field acting on the Co spins.

A more suitable determination of the order of the phase transition in the $Ho(Co_{1-x}Rh_x)_2$ system would be to measure its thermal properties, such as the heat capacity C where a first-order transition is accompanied by a latent heat [$C(T_C) \rightarrow \infty$] and a second-order transition is distinguished by a heat-capacity jump. In this paper, detailed calorimetric measurements are reported in the temperature range 2–100 K with particular attention being paid to the ferromagnetic transition temperature region.

II. SAMPLE PREPARATION AND EXPERIMENTAL TECHNIQUES

Six samples of $Ho(Co_{1-x}Rh_x)_2$ containing 2, 5, 8, 12, 16, and 25 at. % Rh were made in an arc furnace under an argon atmosphere. The resulting buttons of approximately 5-g mass were subsequently heat treated at 800 °C for three weeks. The cubic Laves structure was checked by x-ray powder diffraction. All alloys were single phase except for the 2 and 16 at. % Rh samples which showed impurity phases at less than the 2 at. % level.

The heat capacity of the samples was measured in the temperature range 2–100 K by a pseudo-adiabatic, heat-

pulse technique. The calorimeter[7] consisted of a thermal heat sink and a sample holder inside of a vacuum can. The sample holder is a polished 20-mil-thick, 0.75-in. square of sapphire suspended by cotton thread to a copper support ring which is mechanically anchored to the heat sink by a copper rod. On one side of the sapphire slab, a nichrome film has been deposited for resistive heating of the sample along with an unencapsulated germanium thermometer whose gold electrical leads are silver-epoxied to the sapphire. This arrangement minimizes the heat-capacity contribution to the total measured as well as being constant for each measurement run. The sample is then mounted on the other side of the sapphire by Apiezon grease to ensure good thermal contact. For the $Ho(Co_{1-x}Rh_x)_2$ samples measured, the addenda corrections of the sample holder and grease varied from 2% of the total measured heat capacity for $T<10$ K to less than 10% at ~ 50 K to approximately 20% at the highest temperatures. The Ge thermometer is calibrated *in situ* against a calibrated Ge thermometer over the entire temperature range 2–100 K. To check on the accuracy of the calorimeter, measurements on National Institute of Standards and Technology (NIST) calorimetric copper have been made. The results of these measurements indicate an accuracy of better than 0.5% below 10 K, 1% from 10 to 30 K, and increasing to 5% at the highest temperature.

In addition to the calorimetric measurements, magnetization-versus-temperature curves were measured in fields of 10 Oe using a commercial magnetometer system.[8] Both zero-field-cooled and field-cooled measurements were made in order to determine independently the ferromagnetic and spin-flop transition temperatures for each sample.

III. RESULTS

The total specific heat for the metallic $Ho(Co_{1-x}Rh_x)_2$ alloys consists of several different contributions in addition to the magnetic contribution. These contributions may be written as

$$C=C_e+C_l+C_n+C_m\ , \tag{1}$$

where C_e, C_l, C_n, and C_m represent the electronic, lattice, nuclear, and magnetic contributions, respectively. Typically for metals, the terms C_e, C_l, and C_n can be independently determined from their relative strengths in various temperature regions due to their different temperature dependences. For example, the electronic specific-heat contribution has a linear temperature dependence ($C_e=\gamma T$), the nuclear contribution has a $1/T^2$ dependence ($C_n=A_nT^{-2}$) for temperatures larger than the nuclear energy level splitting, and the lattice contribution has a cubic temperature dependence for temperatures much less than the characteristic Debye temperature Θ_D, i.e., $C_l=\alpha T^3=1944n(T/\Theta_D)^3$ where n is the number of atoms per formula unit.

At very low temperatures ($T<1$ K), the electronic and nuclear contributions are the dominant terms as compared to the lattice contribution in a metal. At higher temperatures ($T>5$ K), the nuclear contribution usually becomes negligible so that a plot of C/T versus T^2 yields a straight-line fit to the data and permits the determination of the γ coefficient (intercept) and the α coefficient (slope). However, in magnetic alloys, the contribution associated with the magnetic interactions or excitations may extend down to 5 K or lower and thus exclude a separate or independent determination of the electronic and lattice coefficients. Such is the situation for $Ho(Co_{1-x}Rh_x)_2$ alloys studied in this paper. Therefore, a different approach to find the various contributions is needed. In order to determine at least three of the four specific-heat contributions for these alloys, one of the contributions must be approximated or deduced from other measurements. From a previous calorimetric measurement on "pure" $HoCo_2$ and $TbCo_2$,[9] a Debye temperature of 256 K was deduced.[10] This value is also very close to the Debye temperature of 266 K for the isomorphic alloy $GdNi_2$.[11] Thus as a first-order approximation for the lattice specific-heat contribution in the $Ho(Co_{1-x}Rh_x)_2$ alloys, a Debye temperature of 256 K is employed. This results in the coefficient α being equal to 0.2196 mJ/K^4 per mole of $Ho(Co_{1-x}Rh_x)_2$ where $n=3$ for these alloys.

At the lowest temperatures ($T<5$ K), the magnetic contribution will be assumed to be negligible as compared to the other contributions and the lattice contribution behaves as T^3. Thus, plots of $(C-C_l)T^2$ versus T^3 should approach straight lines at the lowest temperatures and permit the determination of the nuclear specific-heat coefficient A_n (intercept) and the electronic specific-heat coefficient γ (slope). Figure 1 shows such a plot below 5 K for the five lowest Rh concentrations. Clearly, straight-lines fit can be made for samples with $x\leq 0.12$ as only slight positive deviations are observed at the highest temperatures. These deviations are probably the result of

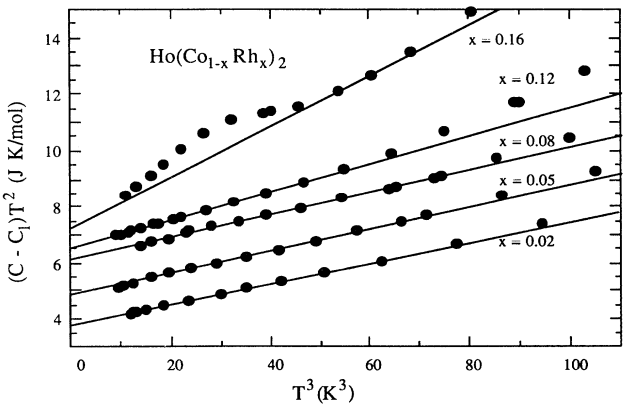

FIG. 1. The nonlattice specific heat of $Ho(Co_{1-x}Rh_x)_2$ alloys plotted as $(C-C_l)T^2$ vs T^3. The origins of the data are displaced successively by 1 J K/mol. The solid lines represent the sum of the nuclear T^{-2} and the electronic T contributions to the specific heat.

the magnetic contribution becoming non-negligible in the 4–5 K temperature range for increasing Rh concentration. The values of A_n and γ determined from these plots are listed in Table I for the various Rh concentrations.

For the $x=0.16$ sample, the data show a small anomaly centered at approximately 3.2 K on top of a straight-line extrapolation from data at a higher, but limited, temperature range 3.7–4.1 K. This anomaly may be due to another small magnetic phase or crystalline phase in this sample. In addition, the straight-line fit probably underestimates A_n and overestimates γ as the magnetic contribution may be very significant in the 3.7–4.1 K temperature range. Already at 4.2 K, a non-negligible magnetic contribution is observed in the data for $x=0.12$ sample and the general trend is for the magnetic contribution to become more prevalent at lower temperatures with increasing Rh concentration. A second factor leading to the overestimation of the γ coefficient is that a $T^{3/2}$ dependence can arise from magnon excitations well below the ferromagnetic Curie temperature and thus may be indistinguishable from the linear T dependence in this limited temperature interval. Thus the A_n and γ coefficients are not very reliable for $x=0.16$. For the $x=0.25$ Rh concentration sample, a larger anomaly is observed below 3.5 K and the resultant $(C-C_1)T^2$ versus T^3 plot did not give rise to any straight-line fit and thus is not shown.

Having obtained values for the nuclear coefficient A_n, it is possible to determine corresponding values for the nuclear hyperfine field $H_{\rm hf}$. In the temperature range $T<5$ K, the nuclear hyperfine specific heat for Ho metal is more than 300 times greater than that for cobalt metal.[12] Thus, the hyperfine field may be considered mainly due to the $4f$ electrons surrounding the ^{165}Ho nuclei. To determine the hyperfine field $H_{\rm hf}$, the following relation is used:

$$H_{\rm hf}=\frac{k_B}{g_N\mu_N}\left[\frac{A_n}{R\left[\frac{1}{3}I(I+1)\right]}\right]^{1/2}, \tag{2}$$

where R is the gas constant, I the nuclear spin, and $g_N\mu_N$ the nuclear magnetic moment of ^{165}Ho ($g_N=1.15$). Having obtained the $H_{\rm hf}$ values, it is then possible to express the nuclear energy splitting Δ in units of temperature by

$$\Delta\ (K)=H_{\rm hf}g_N\mu_N/k_B\ . \tag{3}$$

The values of $H_{\rm hf}$ and Δ (K) are also listed in Table I. For $x\le 0.08$, the values of Δ (K) for the $Ho(Co_{1-x}Rh_x)_2$ alloys are approximately 6% lower than those values determined from heat-capacity measurements on pure Ho ($\Delta=0.319\pm0.003$ K) (Ref. 13) and on $HoCo_2$ ($\Delta=0.316\pm0.005$ K) (Ref. 14) as well as the calculated value of 0.312 ± 0.003 K for Ho (Ref. 15) based on the cubic environment surrounding Ho in the $HoCo_2$ crystal. Furthermore, one notes that for the $x=0.12$ sample, the hyperfine field appears to show a significant decrease as compared to the $H_{\rm hf}$ values for $x\le 0.08$. Also,the value of γ for $x=0.12$ shows about a 25% increase over the γ values for $x\le 0.08$. These γ values of approximately 40 mJ/mol K^2 for $x\le 0.08$ are in excellent agreement with the γ value of 40 mJ/mol K^2 determined in a previous low-temperature calorimetric measurement[14] on pure $HoCo_2$. The even larger γ (=86 mJ/mol K^2) value deduced for the $x=0.16$ sample is probably an overestimation due to the non-negligible magnetic contribution as previously discussed.

The final item listed in Table I is the effective magnetic moment associated with the Ho^{3+} ion. The effective moment can be determined from

$$\mu_p=g\mu_B\langle J_z\rangle\ , \tag{4}$$

where g is the Landé g factor, μ_B the Bohr magneton, and $\hbar\langle J_z\rangle$ the average total angular momentum of the Ho^{3+} ion. To determine $\langle J_z\rangle$, one makes use of the nuclear Hamiltonian

$$\mathcal{H}_N=a_0\mathbf{I}_z+p_0(I_z^2-\tfrac{1}{3}I^2)\ , \tag{5}$$

where a_0 and p_0 are associated with the magnetic dipole and the electric quadrupolar parameters, respectively. The field is applied along the z direction. The magnetic dipole parameter a_0 consists of an extra-ionic term a' and an inter-ionic term a'' which is much smaller than a'. Thus $a_0\approx a'$. Correspondingly, $\langle J_z\rangle$ and a' are related through the formula

$$a'=\frac{\langle J_z\rangle}{J}a_0'\ , \tag{6}$$

where $a_0'=6497$ MHz for Ho^{3+},[16] and the total angular

TABLE I. The electronic γ and nuclear A_n specific-heat coefficients for $Ho(Co_{1-x}Rh_x)_2$ alloys determined in the temperature range 1.5–5.0 K. The nuclear hyperfine splitting $H_{\rm hf}$, the nuclear energy splitting Δ, and the average magnetic moment μ_p for the Ho^{3+} ion are also listed.

x	γ (mJ/mol K^2)	A_n (J K/mol)	$H_{\rm hf}$ (T)	Δ (K)	$\mu_p(Ho^{3+})/\mu_B$
0.02	37.6	3.75	697	0.293	9.39
0.05	40.2	3.81	702	0.295	9.46
0.08	40.4	4.10	728	0.306	9.81
0.12	50.4	3.52	675	0.284	9.10
0.16	86[a]	3.3[a]			

[a]The γ and A_n values for the $x=0.16$ sample are overestimated and underestimated, respectively, due to the non-negligible magnetic specific-heat contribution in this temperature region.

momentum quantum number J is 8 for Ho^{3+}. Thus

$$\mu_p = \mu_B \frac{a'}{a'_0} J \ . \tag{7}$$

The calculated values of μ_p/μ_B for Ho^{3+} are also listed in Table I and vary between 9.39 and 9.81 for $x \leq 0.08$. These compare favorably with $\mu_p = 9.5\mu_B$ for Ho^{3+} in $HoCo_2$ as deduced from neutron-diffraction studies.[17]

Figure 2 shows a plot of the total heat capacity for the $Ho(Co_{0.98}Rh_{0.02})_2$ sample as a function of temperature over the entire temperature range 2–100 K. Two anomalies, one at 18.2 K and the other at 68.1 K are clearly observable. Each anomaly rises very sharply above the "background" specific heat over a narrow temperature interval and appears to be nearly discontinuous, reminiscent of a latent heat. This feature suggests that each anomaly represents a first-order phase transition. Similar sharp heat-capacity anomalies[9] are observed in "pure" $HoCo_2$ at 14 and 75 K. The 14-K anomaly in "pure" $HoCo_2$ represents a spin-flop transition at a temperature T_{sf} as the easy magnetization direction changes from the [110] to the [100] direction as the temperature is raised through T_{sf} (Ref. 18) and the 75-K peak is associated with a first-order ferromagnetic transition. The similarity in these heat-capacity peak suggests that the transition at $T_{sf} = 18.2$ K in the $Ho(Co_{0.98}Rh_{0.02})_2$ sample is a spin-flop transition (first order) with a possible change in the easy-magnetization direction from the [110] to the [100] direction as the temperature is raised while the sharp peak at $T_C = 68.1$ K indicates a transition associated with long-range ferromagnetic ordering.

In order to determine the magnetic contribution to the specific heat and to further distinguish the order at the ferromagnetic transition temperature, it is necessary to subtract the electronic, lattice,and nuclear contributions from the total specific heat,

$$C_m = C - (C_e + C_l + C_n) \ .$$

The coefficients for the electronic and nuclear contributions have been determined from the lowest-temperature data as described previously and so these contributions can be readily subtracted from the total specific heat. The lattice contribution $C_l = 1944n(T/\Theta_D)^3$ is a low-temperature approximation and only valid for the lowest temperatures, $T < 5$ K. For $T > 5$ K, the Debye function must be numerically solved at each temperature according to

$$C_l = 9nR \left[\frac{T}{\Theta_D} \right]^3 \int_0^{y_D} \frac{y^4 e^y dy}{(e^y - 1)^2} \ , \tag{8}$$

where $y_D = \theta_D/T$, $y = \hbar\omega/k_B T$ and $\theta_D = 256$ K. Using the above procedure, C_m has been determined point by point for each sample and is shown in Figs. 3–6 as a function of temperature. C_m for the $x = 0.02$, 0.05, and 0.08 samples (see Fig. 3) increases slightly faster than a linear temperature dependence from the lowest temperatures until the occurrence of the first-order specific-heat peak associated with the spin-flop transition. For all three samples, this peak extends only over a 2-K temperature interval with the value of T_{sf} and the magnitude of $C_m(T_{sf})$ increasing slightly with increasing Rh concentration. For temperatures above T_{sf}, the magnetic specific heat increases until the appearance of a second peak in the 50–65 K range. For the $x = 0.02$ and 0.05 samples, these higher-temperature peaks are very similar in shape to the lower-temperature first-order peaks, in that the magnitude of C_m increases very rapidly in the vicinity of T_C and dC_m/dT (the slope of C_m) approaches an infinite value on either side of T_C. Thus one is led to the con-

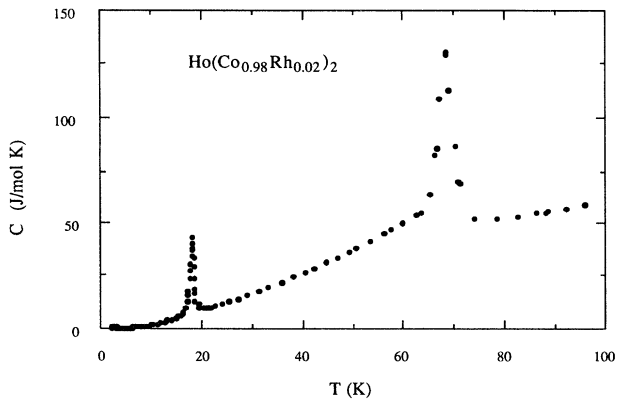

FIG. 2. The total specific heat C for the $Ho(Co_{0.98}Rh_{0.02})_2$ sample in the temperature range 2–100 K.

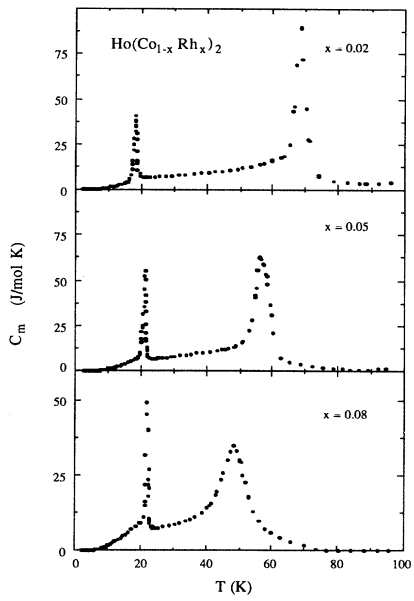

FIG. 3. The magnetic specific heat C_m for $Ho(Co_{1-x}Rh_x)_2$ samples with $x = 0.02$, 0.05, and 0.08 in the temperature range 2–100 K.

clusion that these ferromagnetic transitions are first order in character. However, the character of the higher-temperature peak in the $x=0.08$ sample is less obvious as $C_m(T_C)$ has decreased in magnitude by a factor of 2 ($C_m(T_C)\approx 40$ J/mol K) while the width of the transition is spread over an 8-K temperature interval, nearly the same temperature width as that for the smaller Rh concentration samples. This decrease in height to width gives the appearance of a broaden transition; however, the slope dC_m/dT still has a fairly sharp change from a positive to negative "infinite" value at T_C. Thus the ferromagnetic transition at T_C is also first order in character for the $Ho(Co_{0.92}Rh_{0.08})_2$ alloy, although somewhat broaden. Since the value of T_C is found to decrease with increasing Rh concentration, this suggests that the exchange interaction may be weakening. Another feature of these plots is that C_m approaches zero at the highest temperatures indicating that the determination of the electronic and lattice specific-heat contributions are reasonable.

Figure 4 shows C_m data for the higher Rh concentration samples. Still the first-order specific-heat peak in the vicinity of 20 K is evident for both the $x=0.12$ and 0.16 samples. However, the higher-temperature peak is considerably broaden as compared to the C_m results for the

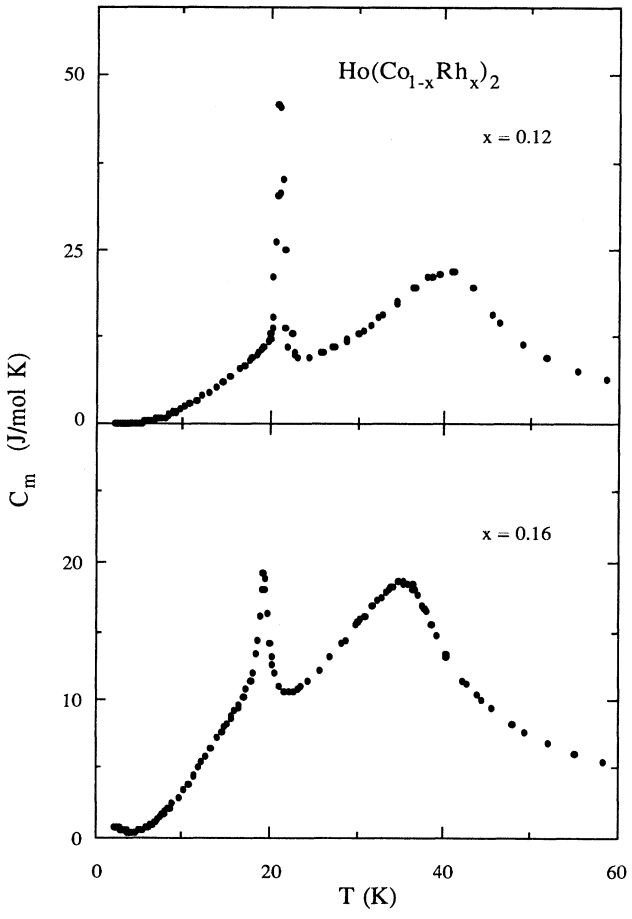

FIG. 4. The magnetic specific heat C_m for $Ho(Co_{1-x}Rh_x)_2$ samples with $x=0.12$ and 0.16 in the temperature range 2–60 K.

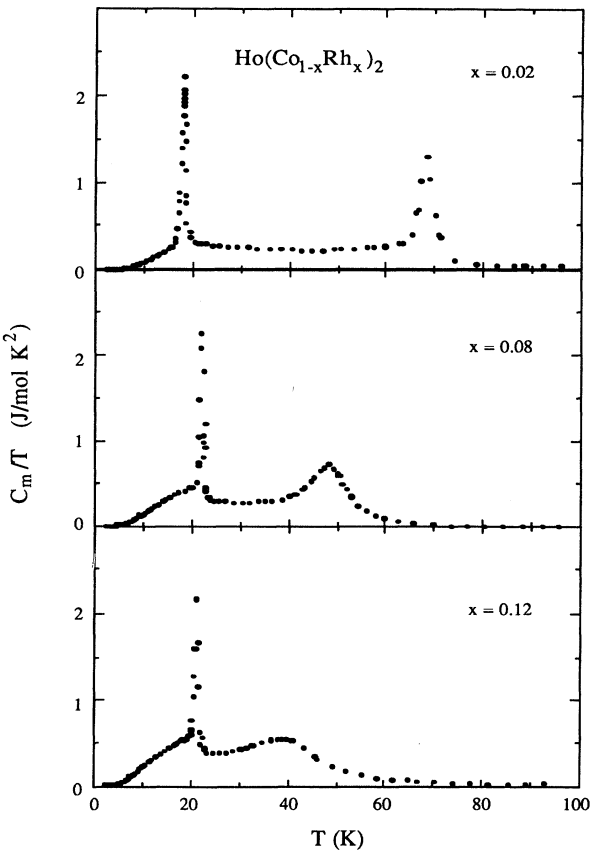

FIG. 5. The magnetic specific heat C_m/T as a function of temperature for $Ho(Co_{1-x}Rh_x)_2$ samples with $x=0.02$, 0.08, and 0.12.

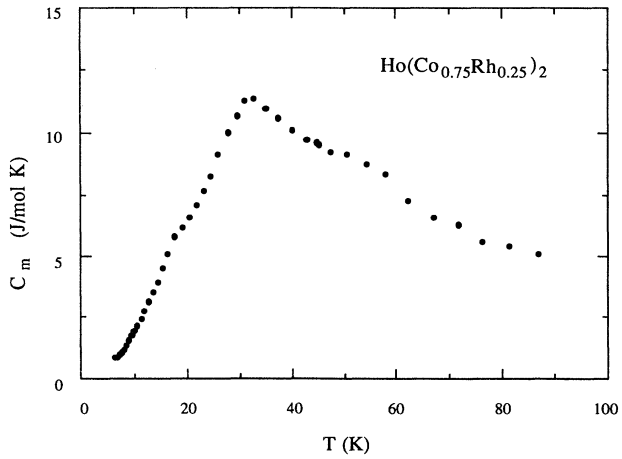

FIG. 6. The magnetic specific heat C_m for the $Ho(Co_{0.75}Rh_{0.25})_2$ sample in the temperature range of 2–100 K.

$x \leq 0.08$ samples as shown by the magnitude of C_m decreasing to approximately 20 mJ/mol K at T_C and the width being essentially indeterminate. Moreover, the slope in the vicinity of T_C has dramatically changed. For $T \leq T_C$, dC_m/dT is positive and decreases to zero as T approaches T_C; however, dC_m/dT is negative and finite for temperatures just above T_C. This characteristic semicusplike behavior is more reminscent of second-order magnetic phase transitions than latent heats associated with first order. Furthermore, this change in the magnetic specific-heat behavior around the vicinity of T_C with increasing Rh concentration is readily visible in C_m/T versus T plots as shown in Fig. 5. Thus we conclude that the ferromagnetic transitions for the $x=0.12$ and 0.16 samples are second order in nature.

The above conclusion that the order of the ferromagnetic transition change from first to second for $x \geq 0.10$ is further supported by determinations of the magnetic entropy from the specific-heat data. The magnetic entropy change can be experimentally determined from the area beneath a C_m/T versus T curve since

$$\Delta S_m = \int_0^T \frac{C_m}{T} dT \ . \tag{9}$$

This determination can then be compared to the maximum entropy change,

$$\Delta S_m(\max) = R \ln(2J+1) = 23.6 \text{ J/mol K} \ , \tag{10}$$

where the total angular momentum $J=8$ since one assumes that the localized magnetic moment is only on the rare-earth ion Ho^{3+}. From plots of C_m/T versus T (see Fig. 5), the magnetic entropy has been determined between 0 and T_C as well as between 0 and 100 K. These entropy determinations as well as T_C and T_{sf} are listed in Table II. The first feature to note from this data is that the measured entropy change up to 100 K is greater than 90% of $\Delta S_m(\max)$. Since C_m/T is vanishingly small even for temperatures just below 100 K, any additional entropy change above 100 K is also extremely small as compared to the measured $\Delta S_m(0-100 \text{ K})$. This means that the magnetic entropy associated with the cobalt moments is very small, much less than the $2(1-x)R \ln(2S+1) = (1-x)11.5$ J/mol K expected from a localized spin $S=\frac{1}{2}$ which would lead to the observed low-temperature moment of one Bohr magneton per Co atom in these alloys.[6] The second feature is that the ratio of $\Delta S_m(0-T_c)/\Delta S_m(0-100 \text{ K})$ is greater than 80% for Rh concentrations of $x \leq 0.08$ and decreases to less than 74% for samples with $x \geq 0.12$. This increased amount of magnetic entropy above T_C is associated with more short-range magnetic ordering occurring above T_C and correspondingly more indicative of second-order magnetic phase transitions. This increased short-range order and the change from first to second order for $x \geq 0.10$ is consistent with magnetization data taken on small pieces from the calorimetric specimens. The temperature width of the spontaneous magnetization changes from a narrow, first-order type for the $x \leq 0.05$ samples to broader transitions with increasing Rh concentration. This change is gradual, thus making it difficult to clearly identify the change in order. However, a clear difference in the reversibility above T_C is seen between samples with $x \leq 0.08$ (reversible) and samples with $x \geq 0.12$ (nonreversible). Figure 7 shows examples of the magnetization as a function of the temperature for the $Ho(Co_{0.92}Rh_{0.08})_2$ and $Ho(Co_{0.88}Rh_{0.12})_2$ alloys, respectively. The magnetization for the $x=0.08$ sample shows a fairly sharp ferromagnetic transition in the 50–57 K temperature region which is reversible and is probably first order in character. Below 51 K, a hysteretic behavior is observed between the zero-field-cooled and field-cooled data. Another strongly hysteretic feature is observed at 21 K which is associated with the spin-flop transition in these polycrystalline samples. Values of the effective magnetic moment and paramagnetic Curie temperature determined from the paramagnetic temperature region are in close agreement with those determined previously.[6] The magnetization data for the $Ho(Co_{0.88}Rh_{0.12})_2$ alloy exhibits a similar characteristic behavior as the data for the $x=0.08$ sample with only a gradual increase in the width of the transition region, thus making it difficult to determine the ex-

TABLE II. The spin-flop transition temperature T_{sf}, the ferromagnetic transition temperature T_C, the order of the magnetic phase transition at T_C, and the magnetic entropy change ΔS in the temperature intervals 0 K $< T \leq$ 100 K and 0 K $< T \leq T_C$ as determined from the magnetic specific-heat data for the $Ho(Co_{1-x}Rh_x)_2$ alloys. These entropy values can be compared to the maximum magnetic entropy change of 23.6 J/mol K calculated from $R \ln(2J+1)$ where $J=8$ for the Ho^{3+} ion. The calculated values of $b_3(T_C)$ and $a_3(T_C)$ from the "*s-d*" model are also listed.

x	T_{sf} (K)	T_C (K)	Order at T_C	ΔS (0–100 K) (J/mol K)	ΔS (0–T_C) (J/mol K)	$b_3(T_C)$ (10^{-14} m^3/mol)	$a_3(T_C)$ (10^{-10} m^3/mol)
0.00	14[a]	75[a]	1st			1.13	−7.913
0.02	18.2±0.1	68.5±0.3	1st	22.6	19.1	1.03	−8.043
0.05	21.2±0.2	56.6±0.4	1st	22.1	17.8	0.854	−8.250
0.08	22.0±0.3	48.6±0.6	1st	20.5	16.5	0.733	−8.367
0.12	21.0±0.3	41.6±1.0	2nd	22.1	16.3	0.627	−8.455
0.16	19.3±0.2	35.8±1.0	2nd	21.5	14.9	0.540	−8.518
0.25	18.4±0.4	31.6±1.0	2nd	18.7	7.6	0.477	−8.557

[a]From Ref. 9.

act nature of the order. However, the nonreversible, hysteretic behavior above T_C is evident which may be suggestive of a second-order transition with more short-range order between the magnetic moments above T_C.

The specific-heat peaks associated with the spin-flip and ferromagnetic transitions in the $x=0.25$ sample are less pronounced as shown in Fig. 6. The corresponding peaks centered at 18.4 and 31.6 K are very broad even for second-order transitions. Furthermore, another broad anomaly is observable in the 45–70 K temperature range which may result from another magnetic phase transition. Although the x-ray-diffraction pattern indicates a single-crystalline phase material, it is possible that inhomogeneities in the Rh concentration exists in the interior of the sample causing the presence of a higher-temperature ferromagnetic phase(s). This anomalous behavior is also seen in the magnetization data which further supports the inhomogeneity hypothesis.

Finally, Fig. 8 shows the dependence of T_C and T_{sf} upon the Rh concentration as determined from the present calorimetric investigation as well as from the earlier magnetization study.[6] A strong deviation from a linear decrease in T_C with Rh concentration is seen for $x \geq 0.1$ while T_{sf} is a maximum at $x \approx 0.1$. Both of these trends are consistent with a change in the character of the order at $x \approx 0.1$. In addition, there is remarkably good agreement between both sets of T_C values, especially considering the difficulty in determining the ferromagnetic Curie temperature from a broad transition in the magnetization data. Choosing the temperature where our zero-field-cooled magnetization exhibits its first maximum with decreasing temperature as T_C and the temperature of the sharp field-cooled magnetization minimum in the 20-K temperature vicinity as T_{sf}, better agreement can be found between the calorimetric and magnetically determined critical temperatures.

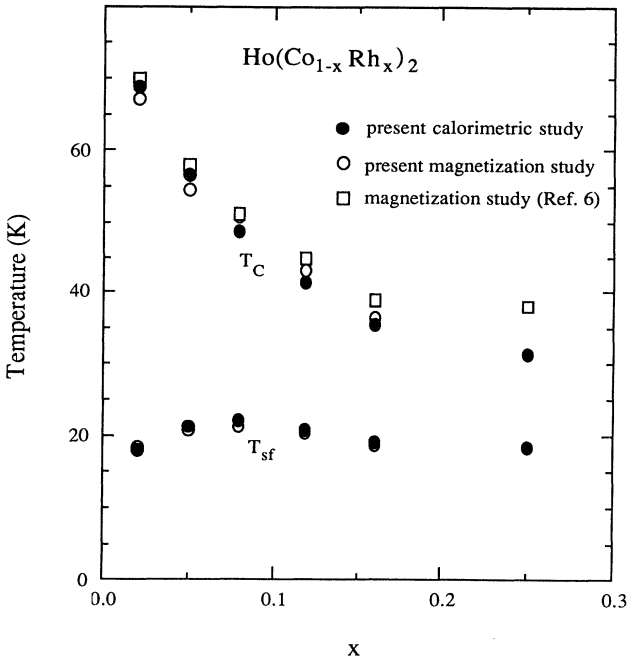

FIG. 8. The spin-flip transition temperature T_{sf} and the ferromagnetic Curie temperature T_C as determined from calorimetric and magnetic measurements on the $Ho(Co_{1-x}Rh_x)_2$ system.

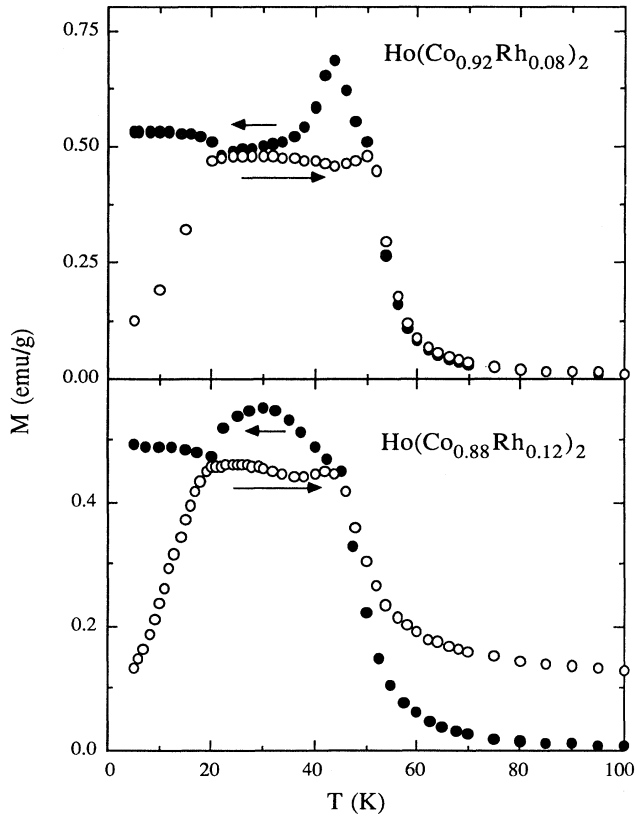

FIG. 7. The temperature dependence of the zero-field-cooled (○) and the field-cooled (●) magnetization M for the $Ho(Co_{0.92}Rh_{0.08})_2$ and $Ho(Co_{0.88}Rh_{0.12})_2$ samples.

IV. DISCUSSION

The model which is generally used to analyze the magnetic phase transition at T_C is the "*s-d*" model as proposed initially by Bloch and Lemaire.[5] This model has been previously used to explain the different order of the ferromagnetic phase transitions in RCo_2 alloys.[19,20] The model, as applied to the $Ho(Co_{1-x}Rh_x)_2$ alloys, assumes that the localized $4f$ electrons of the holmium atoms interact with the itinerant $3d$ electrons on the cobalt atoms. According to the Landau theory, if the free energy F is expanded in terms of the total magnetization of the rare-earth and cobalt atoms,

$$F = C_1(T)\frac{M^2}{2} + C_3(T)\frac{M^4}{4} + C_5(T)\frac{M^6}{6} + \cdots , \qquad (11)$$

then the order of the magnetic phase transition is indicat-

ed by the sign of $C_3(T_C)$. If the sign of $C_3(T_C)$ is negative, the transition is first order; alternatively, if the sign of $C_3(T_C)$ is positive, the transition is second order.

In the "*s-d*" model, the value of $C_3(T_C)$ is obtained from

$$C_3(T_C)=\frac{\{b_3(T_C)+a_3(T_C)[\chi_d(T_C)\hat{J}]^4\}}{[1+\chi_d(T_C)\hat{J}]^4}\ , \tag{12}$$

where χ_d is the paramagnetic susceptibility of the itinerant $3d$ electrons, $\hat{J}$ is the molecular field coefficient between the spins of the cobalt $3d$ electrons and the spins of the holmium $4f$ electrons. From published data[4,5,19] on $HoCo_2$,

$$b_3(T_C)=1.51\times10^{-16}T_C\ (\mathrm{m^3/mol}) \tag{13}$$

and

$$a_3(T_C)=\left[-8.696\times10^{-10}\ \frac{\mathrm{m^3}}{\mathrm{mol}}\right]\left[1-\left[\frac{T_C}{250}\right]^2\right]. \tag{14}$$

For the $Ho(Co,Rh)_2$ system, the calculated values for $b_3(T_C)$ and $a_3(T_C)$ are listed in Table II using the T_C values determined from this calorimetric measurement. Clearly, $b_3(T_C)$ is positive-definite, $a_3(T_C)$ is negative since $T_C\leq75$ K, and the magnitude of $b_3(T_C)$ is less than that of $a_3(T_C)$. Thus the sign of $C_3(T_C)$ and correspondingly the order of the transition is mainly determined by the magnitude of the product $\chi_d\hat{J}$. From published values of χ_d ($=49\times10^{-9}$ $\mathrm{m^3/mol}$) and $\hat{J}$ ($=-2.2\times10^6$ $\mathrm{mol/m^3}$) for $HoCo_2$,[5] the product $\chi_d\hat{J}$ is equal to -0.11 and the value of $C_e(T_C)$ is -16×10^{-14} $\mathrm{m^3/mol}$, which is in accord with the idea that a negative value of $C_3(T_C)$ is indicative of a first-order transition in this model. In order for $C_3(T_C)$ to become positive $C_3(T_C)\geq0$ or alternatively $b_3(T_C)\geq-a_3(T_C)(\chi_d\hat{J})^4$ in the $Ho(Co,Rh)_2$ system, the product $\chi_d\hat{J}$ must decrease by approximately 50%.

To determine whether the collective behavior of the $3d$ electrons or the exchange between the $3d$ electrons and the localized $4f$ spins is more responsible for the change in the order of the magnetic transition, high-temperature magnetization studies are typically performed in order to determine the values of χ_d and $\hat{J}$ as a function of the Rh substitution. However, it should be noted that the paramagnetic susceptibility χ_d is related to the electronic specific-heat coefficient γ as follows:

$$C_e=\gamma T=\tfrac{1}{3}\pi^2\mathcal{D}(E_F)k_B^2T \tag{15}$$

and

$$\chi_d=\frac{\mu^2 3\mathcal{D}(E_F)}{\pi^2k_B^2}\ , \tag{16}$$

so

$$\chi_d=\frac{\mu^2 3\gamma}{\pi^2k_B^2}\ , \tag{17}$$

where $\mathcal{D}(E_F)$ is the density of electron states at the Fermi energy E_F, and μ is the magnetic moment of the d electrons. Thus χ_d is directly proportional to the magnitude of γ. As seen in Table I, the electronic specific-heat coefficient γ only shows a slight increase as the rhodium concentration increases from $x=0.02$ to 0.08; however, an approximate 25% increase in the γ value is observed for the $x=0.12$ sample. Thus as the Rh concentration increases, one would expect χ_d to exhibit a similar increase with Rh concentration and correspondingly not be responsible for the 50% decrease in the $\chi_d\hat{J}$ product necessary for changing the sign of $C_3(T_C)$. Thus the change from a first- to second-order ferromagnetic transition for $x\geq0.10$ in the $Ho(Co_{1-x}Rh_x)_2$ alloys is probably due to the strength of the exchange interactions becoming increasingly weaker as the Rh concentration is increased. This conclusion is in agreement with a prior magnetization study[6] on the $Ho(Co_{1-x}Rh_x)_2$ system. Although an approximate 20% decrease in the value of χ_d and a 20% decrease in the $\hat{J}$ value were deduced from the data for a $x=0.08$ sample to $x=0.16$ and 0.25 samples, the magnetic data for the $x=0.16$ was rather poor and thus only indicated a trend.

V. CONCLUSIONS

The magnetic specific heat for $Ho(Co,Rh)_2$ as a function of Rh concentration has been measured in the temperature range 2–100 K. For $x\leq0.16$, two specific-heat anomalies are observed. The lower-temperature anomaly retains a first-order character and is related to a change in the easy-magnetization direction (spin-flop transition). The temperature T_{sf} at which this transition occurs initially increases from 18.2 K to about 21.3 K as x is increased from 0.02 to 0.08 and then it decreases to 19.4 K as x increases to 0.16. The higher-temperature anomaly is related to a ferromagnetic phase transition at a Curie temperature T_C with T_C decreasing with increasing Rh concentration. This transition is definitely first order for $x\leq0.08$. However, for $x\geq0.12$, the order of the transition is less certain as the temperature width associated with the transition broadens and the curvature of the magnetic specific heat around T_C changes. This broadening with a change in the curvature around T_C and the appearance of a significant increase in the amount of magnetic entropy occurring above T_C due to short-range magnetic ordering suggests that the order of the ferromagnetic transition is second order for alloys with $x\geq0.10$. The specific-heat data also indicates that the magnetic effects in $Ho(Co_{1-x}Rh_x)_2$ alloys are primarily due to the Ho atoms since (i) the values of Δ (K) and μ_p determined from nuclear specific-heat data compare favorably to those values for Ho in pure $HoCo_2$ and (ii) the total magnetic entropy change from 0 to 100 K is consistent with the theoretical maximum of $R\ln(2J+1)$ for just the Ho^{3+} ions. Finally, utilizing the "*s-d*" model in conjunction with the specific-heat data suggests that the change from first to second order in the ferromagnetic transition with increasing Rh content is due to a reduction in the magnetic exchange interactions between the Ho $4f$ magnetic moments and the cobalt $3d$ electrons.

[1]D. Bloch, D. M. Edwards, M. Shimizu, and J. Voiron, J. Phys. F **5**, 1217 (1975).
[2]R. Lemaire, Cobalt **33**, 201 (1966).
[3]A. Tari, J. Magn. Magn. Mater. **30**, 209 (1982).
[4]T. D. Hien, N. H. Duc, and J. J. M. Franse, J. Magn. Magn. Mater. **54-57**, 471 (1986).
[5]D. Bloch and R. Lemaire, Phys. Rev. B **2**, 2648 (1970).
[6]A. Tari, J. Magn. Magn. Mater. **69**, 247 (1987).
[7]G. W. Hunter, Ph.D. thesis Wayne State University, 1987 (unpublished).
[8]Model MPMS, by Quantum Design, San Diego, CA.
[9]J. Voiron, A. Berton, and J. Chaussy, Phys. Lett. **50A**, 17 (1974).
[10]Debye temperature was actually determined from calorimetric measurements on YCo_2. See Ref. 5 and K. Ikeda, K. A. Gschneidner, R. J. Stierman, T.-W. E. Tsang, and O. D. McMasters, Phys. Rev. B **29**, 5039 (1984).
[11]J. A. Cannon, J. I. Budnick, R. S. Craig, S. G. Sankar, and D. A. Keller, in *Magnetism and Magnetic Materials, Denver, 1972,* Proceedings of the 18th Annual Conference on Magnetism and Magnetic Materials, AIP Conf. Proc. No. 10, edited by C. D. Graham and J. J. Rhyne (AIP, New York, 1973), Vol. 2, p. 905.
[12]W. Proctor, R. G. Scurlock, and E. M. Wray, Phys. Lett. **20**, 621 (1966); K. N. R. Taylor and J. T. Christopher, J. Phys. C **2**, 2237 (1969); O. V. Lounasmaa, Phys. Rev. **128**, 1136 (1962).
[13]M. Krusius, A. C. Anderson, and B. Holstrom, Phys. Rev. **177**, 910 (1969).
[14]D. Bloch, J. Voiron, A. Berton, and J. Chaussy, Solid State Commun. **12**, 685 (1973).
[15]B. Bleaney, J. Appl. Phys. **34**, 1024 (1963).
[16]B. Bleaney, in *Magnetic Properties of Rare Earth Metals,* edited by R. J. Elliot (Plenum, London, 1972), Chap. 8.
[17]D. Gignoux, F. Givord, and J. Schweizer, J. Phys. F **7**, 1823 (1977).
[18]D. Gignoux, F. Givord, and R. Lemaire, Phys. Rev. B **12**, 3878 (1975).
[19]D. Bloch, D. M. Edwards, M. Shimizu, and J. Voiron, J. Phys. F **5**, 1217 (1975).
[20]J. Inoue and M. Shimizu, J. Phys. F **12**, 1811 (1982).